



Diagnostic accuracy of *anti*-3-[¹⁸F]-FACBC PET/MRI in gliomas

Anna Karlberg^{1,2} · Lars Kjelsberg Pedersen³ · Benedikte Emilie Vindstad² · Anne Jarstein Skjulsvik^{4,5} · Håkon Johansen¹ · Ole Solheim^{6,7} · Karoline Skogen⁸ · Kjell Arne Kvistad¹ · Trond Velde Bogsrud^{9,10} · Kristin Smistad Myrmet¹¹ · Guro F. Giskeødegård¹² · Tor Ingebrigtsen^{3,13} · Erik Magnus Berntsen^{1,2} · Live Eikenes²

Received: 22 June 2023 / Accepted: 6 September 2023 / Published online: 30 September 2023
© The Author(s) 2023

Abstract

Purpose The primary aim was to evaluate whether *anti*-3-[¹⁸F]FACBC PET combined with conventional MRI correlated better with histomolecular diagnosis (reference standard) than MRI alone in glioma diagnostics. The ability of *anti*-3-[¹⁸F]FACBC to differentiate between molecular and histopathological entities in gliomas was also evaluated.

Methods In this prospective study, patients with suspected primary or recurrent gliomas were recruited from two sites in Norway and examined with PET/MRI prior to surgery. *Anti*-3-[¹⁸F]FACBC uptake (TBR_{peak}) was compared to histomolecular features in 36 patients. PET results were then added to clinical MRI readings (performed by two neuroradiologists, blinded for histomolecular results and PET data) to assess the predicted tumor characteristics with and without PET.

Results Histomolecular analyses revealed two CNS WHO grade 1, nine grade 2, eight grade 3, and 17 grade 4 gliomas. All tumors were visible on MRI FLAIR. The sensitivity of contrast-enhanced MRI and *anti*-3-[¹⁸F]FACBC PET was 61% (95%CI [45, 77]) and 72% (95%CI [58, 87]), respectively, in the detection of gliomas. Median TBR_{peak} was 7.1 (range: 1.4–19.2) for PET positive tumors. All CNS WHO grade 1 pilocytic astrocytomas/gangliogliomas, grade 3 oligodendrogliomas, and grade 4 glioblastomas/astrocytomas were PET positive, while 25% of grade 2–3 astrocytomas and 56% of grade 2–3 oligodendrogliomas were PET positive. Generally, TBR_{peak} increased with malignancy grade for diffuse gliomas. A significant difference in PET uptake between CNS WHO grade 2 and 4 gliomas ($p < 0.001$) and between grade 3 and 4 gliomas ($p = 0.002$) was observed. Diffuse IDH wildtype gliomas had significantly higher TBR_{peak} compared to IDH1/2 mutated gliomas ($p < 0.001$). Adding *anti*-3-[¹⁸F]FACBC PET to MRI improved the accuracy of predicted glioma grades, types, and IDH status, and yielded 13.9 and 16.7 percentage point improvement in the overall diagnoses for both readers, respectively.

Conclusion *Anti*-3-[¹⁸F]FACBC PET demonstrated high uptake in the majority of gliomas, especially in IDH wildtype gliomas, and improved the accuracy of preoperatively predicted glioma diagnoses.

Clinical trial registration ClinicalTrials.gov ID: NCT04111588, URL: <https://clinicaltrials.gov/study/NCT04111588>

Keywords *Anti*-3-[¹⁸F]FACBC · PET · MRI · Glioma

Introduction

About one-third of primary brain tumors are malignant, and of these gliomas account for about 80% [1–3]. Epidemiological studies report incidence rates of gliomas from 4.8 to 7.7/100,000 per year [4]. In Norway, around 320 patients

are diagnosed with diffuse gliomas each year [5]. Gliomas are classified according to the 2021 World Health Organization (WHO) classification of tumors of the central nervous system (CNS), based on histopathological and molecular features. The majority of malignant primary brain tumors are adult-type diffuse gliomas, which are now classified into three categories: isocitrate dehydrogenase (IDH) mutant astrocytomas (CNS WHO grade 2–4), IDH-mutant and 1p/19q co-deleted oligodendrogliomas (CNS WHO grade 2–3), and IDH-wildtype (IDHwt) glioblastomas (CNS WHO grade 4) [6, 7]. Tumor classification is essential for treatment decisions, and for estimation of treatment response and overall prognosis [8, 9].

Erik Magnus Berntsen and Live Eikenes have contributed equally to this work.

✉ Anna Karlberg
annamka@stud.ntnu.no

Extended author information available on the last page of the article

The recommended diagnostic imaging modality for glioma detection according to present guidelines is magnetic resonance imaging (MRI), including T2-weighted, T2-weighted fluid-attenuated inversion recovery (FLAIR), pre- and post-contrast enhanced 3D T1 sequences and diffusion-weighted imaging (DWI) [10]. Perfusion-weighted imaging is optional but may be beneficial, especially in the assessment of low-grade gliomas [11]. The gold standard for diagnosis, however, remains histomolecular analysis of tumor tissue, which requires operative biopsy sampling. Due to gliomas' heterogenous nature, tissue sampling might result in underestimation of tumor grade or misdiagnosis, as some tumors have malignant foci, not visible with conventional imaging [12–14].

Radiolabeled amino acids (AAs) are important imaging agents for positron emission tomography (PET) diagnostics due to the increased levels of AA transport that occur in many tumor cells compared to normal tissue [15]. A wide range of AA tracers have been developed for clinical PET imaging of oncological diseases such as brain tumors, neuroendocrine tumors, and prostate cancer [16]. The AA PET tracers [methyl- ^{11}C]-L-methionine (^{11}C MET), O-(2- ^{18}F -fluoroethyl)-L-tyrosine (^{18}F FET), and 3,4-dihydroxy-6- ^{18}F fluoro-L-phenylalanine (^{18}F FDOPA) are recommended by current international guidelines to improve brain tumor diagnostics, resection, tissue sampling, grading, treatment planning and therapy response assessment [17, 18]. The longer half-life of ^{18}F -labeled tracers (110 min) compared to ^{11}C -labeled tracers (20 min) facilitates the utility of AA tracers in hospitals without on-site radiopharmaceutical production [16].

Anti-1-amino-3- ^{18}F -fluorocyclobutane-1-carboxylic acid (*anti*-3- ^{18}F FACBC) is an AA PET tracer with favorably low uptake in normal brain tissue, resulting in higher tumor-to-background ratio (TBR) compared to the current recommended tracers [19, 20]. *Anti*-3- ^{18}F FACBC is further mediated not only via leucine preferring transport system L (LAT1), like the above mentioned tracers, but also via alanine-serine-cysteine transporter 2 (ASCT2) which is commonly upregulated in cancer cells [16, 21, 22]. Previous studies have shown *anti*-3- ^{18}F FACBC uptake in gliomas of various grades and types, all with the common conclusion that PET with this tracer is effective in the detection of gliomas, and may add complementary information, especially in tumor regions not visualized with contrast-enhanced MRI [23–26]. It has also been suggested that *anti*-3- ^{18}F FACBC can discriminate between low- and high-grade gliomas [27].

Even though *anti*-3- ^{18}F FACBC was originally developed for brain tumor imaging over twenty years ago [28], it has not been widely used or implemented in current guidelines for this purpose. Instead, the tracer has been more commonly used in biochemical recurrent prostate cancer [29].

More studies are therefore needed to establish the potential role of *anti*-3- ^{18}F FACBC PET in glioma diagnostics. It is of special interest to investigate whether *anti*-3- ^{18}F FACBC PET can differentiate between tumor grades and subtypes, to increase the accuracy of noninvasive diagnostics.

The aim of this study was to evaluate whether addition of *anti*-3- ^{18}F FACBC PET to conventional MRI could improve diagnostic accuracy for patients with primary and recurrent gliomas. We also evaluated the ability of *anti*-3- ^{18}F FACBC to differentiate between histopathological and molecular entities in gliomas.

Materials and methods

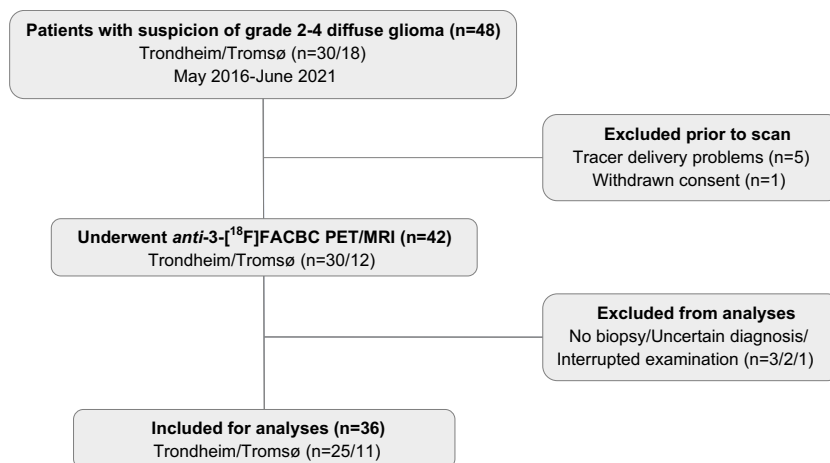
Study design

This is a prospective diagnostic accuracy study evaluating *anti*-3- ^{18}F FACBC PET (index test) alone and as a supplement to conventional MRI towards histomolecular analysis (reference standard). The standards for reporting of diagnostic accuracy studies (STARD) guided the conduct and reporting [30].

Subjects

Adult patients (> 16 years) with suspicion of primary or recurrent grade 2–4 diffuse glioma ($n=48$) were recruited from the Department of Neurosurgery, St. Olavs Hospital, Trondheim University Hospital, Trondheim, and from the Department of Neurosurgery, University Hospital of North Norway, Tromsø, between May 2016 and June 2021. Patient selection was based on convenience sampling. Exclusion criteria were pregnancy, breastfeeding, pacemakers, or defibrillators not compatible with 3 T (T) MRI, preclusion to consent (e.g., due to severe dysphasia or cognitive deficits), weight > 120 kg, and/or Karnofsky performance status ≤ 60 . Six patients were excluded prior to PET/MRI examination due to tracer delivery problems or withdrawn consent, and 42 underwent a pre-surgical *anti*-3- ^{18}F FACBC PET/MRI examination. Patients with no biopsy, uncertain histomolecular diagnosis, or interrupted examination were excluded from analyses. However, patients with grade 1 gliomas scheduled for treatment based on suspicion of being diffuse gliomas (grade 2–4) were not excluded since we wanted to evaluate the potential of *anti*-3- ^{18}F FACBC also for such a clinical reality. This left data from 36 patients (15 females/21 males, 24 primary gliomas/12 recurrent gliomas) available for data analyses (Fig. 1). Average age was 47 (range 16–80) years.

Fig. 1 Inclusion/exclusion flow-chart for patients in the study



Histomolecular analysis

The histomolecular diagnoses were determined according to the 2021 WHO Classification of Tumors of the Central Nervous System [7], including 1p/19q codeletion status; IDH-, TP53-, and ATRX-mutation status; MGMT- and TERT-promotor methylation status; CDKN2A/B homozygous deletion, and Ki67 labelling index. Molecular parameters were not systematically and identically tested for all tumors (except for IDH mutation status), but evaluated for all cases where it was diagnostically relevant to complement the diagnoses based on histopathology. Full description of the histomolecular examinations is found in Supplementary Information 1. The histomolecular diagnoses were used as reference throughout the analyses.

Imaging protocol

PET/MRI acquisition

Patients were examined on two identical PET/MRI systems (Siemens Biograph mMR, software version Syngo MR VE11P (Prior to May 2017: B20P), Erlangen, Germany). The patients received an intravenous injection of *anti*-3-[¹⁸F]FACBC (fluciclovine (¹⁸F)) (3.0 ± 0.2 MBq/kg) at the onset of a 45-min one-bed listmode PET acquisition.

Standard MRI sequences, according to current consensus recommendation on standardized brain tumor imaging protocols [10, 11], were acquired simultaneously. These included pre- and post-contrast enhanced (ce) 3D T1 magnetization prepared rapid gradient echo imaging (MPRAGE), 3D FLAIR, and axial T2, DWI, and dynamic susceptibility contrast (DSC) perfusion imaging. An ultrashort echo time (UTE) sequence for attenuation correction purposes was also acquired.

One patient (ID_07) was scanned on a PET/CT system (Siemens Biograph 128 Vision 600 Edge, software version

VG76A) and the next day on a stand-alone MRI system (Siemens Skyra, software version Syngo MR E11) due to technical problems with the PET/MRI system.

PET reconstruction

The last 15 min of the PET acquisition (30–45 min post injection (p.i)) were used to reconstruct static PET images (for one patient (ID_20), 42–57 min p.i was used due to severe anxiety and movement during imaging). For dynamic analyses, data were reconstructed into 12×5 s, 6×10 s, 6×30 s, 5×60 s, and 7×300 s time frames. Iterative reconstruction (3D ordered subset expectation maximization (OSEM), 3 iterations, 21 subsets, 344×344 matrix, 4 mm Gaussian post filter) with point spread function (PSF), decay-, scatter-, and attenuation-correction (AC) was performed. AC was based on the UTE sequence together with the deep learning method DeepUTE developed by Ladefoged et al. [31, 32]. For five patients scanned prior to May 2017, the regular UTE sequence was used for attenuation correction.

Image interpretation and reporting

Initial PET and MRI readings

PET and MRI readings were performed by experienced nuclear medicine physicians (H.J: 5 y, T.V.B: 20 y) and neuroradiologists at each site, as a part of clinical routine. Tumors were defined by nuclear medicine physicians as “PET positive” if the visual uptake of *anti*-3-[¹⁸F]FACBC in the tumor was higher than in the surrounding tissue. Sensitivities with 95% confidence intervals (CIs) to detect gliomas were calculated for MRI FLAIR, ce-MRI, and PET.

Systematic, retrospective MRI readings

Extended, systematic retrospective MRI readings were performed by another two experienced neuroradiologists (10- and 25-years' experience) using Sectra picture archiving system (PACS) system.

The purpose was to evaluate how good the estimated diagnosis was, based on routine MRI sequences only (3D T1 pre- and post-contrast, 3D FLAIR, axial T2, DWI, and DSC) compared to the gold standard histomolecular diagnosis. Apparent diffusion coefficient (ADC) maps were calculated from the DWI, and relative cerebral blood volume (rCBV) was calculated from the DSC perfusion imaging (Siemens syngo.via, VB60A).

The readers were blinded for the histomolecular results, previous radiological assessments, and PET data. The only available information was patients' age and whether the tumors were untreated or recurrent. Both readers were familiar with the 2021 WHO Classification of tumors of the CNS [7], and three recent articles discussing its neuroradiological implications [33–35].

Systematic MR imaging characteristics for evaluation of diagnostic traits in the reading scheme were predominantly cortical based (Y/N), ring contrast enhancement (Y/N), patchy contrast enhancement (Y/N), central necrosis (Y/N), T2/FLAIR mismatch (Y/N), increased rCBV (Y/N), and indirect signs of calcification (Y/N). ADC were also assessed by both readers. Following this quantitative evaluation, the estimated glioma grade and molecular subtype were predicted by the two readers.

Thereafter, the aim was to evaluate if the estimated diagnostic accuracy could have been improved by adding *anti-3-¹⁸F* FACBC PET to their MRI readings, by using the known imaging characteristics found in this study for this tracer (TBR_{peak} threshold values established by receiver operator characteristics (ROC) curve analyses, see “[Statistical analysis](#)”).

Quantitative image analysis

PMOD (software version 4.304, PMOD Technologies LLC, Zürich, Switzerland) was used for all quantitative image analyses. All ce-MRI as well as static and dynamic PET datasets were rigidly co-registered to the corresponding MRI FLAIR images to assure proper alignment between all datasets. For dynamic datasets, the last 5-min frame was used for registration and the same transformation matrix was then applied for all other time frames.

MRI tumor volumes (FLAIR and ce-MRI) were defined by a neuroradiologist and a physicist together. For each tumor, a large spherical volume of interest (VOI) was placed manually to cover the whole tumor. Image threshold values were subsequently adjusted to separately segment the

visual high intensity regions in the FLAIR images and the contrast-enhanced regions from ce-MRI. In a few patients with contrast-enhancing tumors and surrounding areas with high FLAIR-intensity, the latter was considered peri-tumoral vasogenic edema, and excluded from the tumor volumes.

For static PET images and PET positive tumors, VOIs covering the whole tumor uptake were drawn. Thereafter, maximum standardized uptake values (SUV_{max}) and peak VOIs of 1 mL with the highest uptake within the volumes (SUV_{peak}) were selected automatically by the software. For PET negative tumors, SUV_{peak} was defined as the average SUV within the MRI FLAIR tumor volumes. SUV_{max} for negative tumors was not defined, due to spill-in effects from surrounding healthy tissue within the FLAIR tumor volumes, causing large uncertainties in the estimated activity uptake. Tumor-to-background ratios for the peak values (TBR_{peak}) were therefore used for all image analyses of static PET images. TBR_{peak} was calculated using normal brain uptake as reference. The reference uptake region was defined in the contra-lateral side of the brain, above the ventricles, consisting of six consecutive, crescent shaped regions of interest (ROIs), forming a VOI, to assess the background activity (SUV_{background}), as described by Unterrainer et al. [36].

Dynamic analyses were performed for all PET positive tumors ($n=26$), using the same peak VOIs as for the static analyses according to international guidelines [18].

Statistical analysis

SPSS (IBM SPSS Statistics, version 27) was used for all statistical calculations. To compare differences in TBR_{peak} across glioma grades (2/3/4) and glioma types (astrocytoma/oligodendroglioma/glioblastoma), a Kruskal-Wallis H test was performed with a post-hoc Mann-Whitney *U* test. The Mann-Whitney *U* test was also used for comparisons of TBR_{peak} between primary and recurrent gliomas, and between gliomas with different IDH status. Grade 1 gliomas differ in characteristics compared to adult-type diffuse gliomas, both clinically and in histopathological and molecular features, and they were therefore not included in the statistical comparative analyses.

The inter-rater agreement for the extended MRI readings was evaluated using Cohen's Kappa statistics for dichotomous “yes/no”-data. Kappa values ($\kappa \leq 0.20$, 0.21–0.39, 0.40–0.59, 0.60–0.79, 0.80–0.90, and > 0.9) were considered as *no*, *minimal*, *weak*, *moderate*, *strong* and *almost perfect* agreement, respectively [37]. For ADC values, intraclass correlation coefficient (ICC) with a two-way random-effects model and absolute agreement definition was used. ICC values < 0.5 , 0.5–0.75, 0.75–0.9, and > 0.90 were indicative of *poor*, *moderate*, *good*, and *excellent* reliability, respectively [38].

Receiver operator characteristics (ROC) curve analyses were used to find optimal TBR_{peak} threshold values between different glioma grades, types and IDH status. The following classification was used for area under the curve (AUC) discrimination: $AUC < 0.5$ was considered as *none*, $0.5 \leq AUC < 0.7$ as *poor*, $0.7 \leq AUC < 0.8$ as *acceptable*, $0.8 \leq AUC < 0.9$ as *excellent*, and ≥ 0.9 as *outstanding* [39]. The established threshold values were then used to evaluate if *anti*-3- $[^{18}F]$ FACBC PET could improve the accuracy of the radiological diagnoses based on MRI only (the extended MRI readings by two neurologists). In all statistical analyses, $p \leq 0.05$ was considered statistically significant.

Ethics approval

The study was approved by the Regional Ethics Committee (REC Central Norway, reference numbers 2016/279 and 2018/2243). Results from nine of the first patients examined prior to Nov. 2017 (2016/279) have been published previously [24, 40]. All patients signed written informed consent.

Results

Histomolecular analysis

Histomolecular analysis revealed two CNS WHO grade 1 gliomas (pilocytic astrocytoma and/or ganglioglioma $n = 2$), nine grade 2 gliomas (astrocytoma $n = 3$, oligodendroglioma $n = 6$), eight grade 3 gliomas (astrocytoma $n = 5$, oligodendroglioma $n = 3$), and 17 grade 4 gliomas (astrocytoma $n = 2$, glioblastoma $n = 15$). Further analyses of genes and molecular profiles are summarized in Supplementary Information 2. To facilitate reading, “CNS WHO grade” is further referred to as “grade.”

Image interpretation

MRI

All 36 (100%) tumors were visible on MRI FLAIR, and 22/36 had contrast-enhanced regions (all grade 1 tumors, none grade 2 tumors, 4/8 grade 3 tumors, and 16/17 grade 4 tumors), yielding a sensitivity of 61% (95%CI [45, 77]) for ce-MRI in the detection of gliomas. MRI FLAIR volumes ranged from 1.4 to 167.9 mL, and ce-MRI volumes from 0.03 to 27.1 mL (Supplementary Information 2).

PET

PET was reported positive in 26/36 tumors, yielding an overall sensitivity of 72% (95%CI [58, 87]) for *anti*-3- $[^{18}F]$ FACBC in the detection of gliomas. As shown in Fig. 2,

all grade 1 pilocytic astrocytomas and gangliogliomas were PET positive, as well as all grade 3 oligodendrogliomas and all grade 4 astrocytomas and glioblastomas. None of the grade 2 astrocytomas had PET uptake. A larger fraction of grade 2 and 3 oligodendrogliomas (55.6%) were PET positive compared to grade 2 and 3 astrocytomas (25.0%) (Supplementary Information 2). All tumors with contrast-enhancement on MRI were PET positive, while 4/26 (15.4%) of PET positive tumors did not show contrast enhancement on MRI (Patients: ID_10 with grade 2 oligodendroglioma, ID_11 with grade 2 oligodendroglioma, ID_17 with grade 3 oligodendroglioma, and ID_25 with grade 4 glioblastoma).

Quantitative image analysis

Anti-3- $[^{18}F]$ FACBC uptake versus glioma grades, types, and molecular features

Median TBR_{peak} was 7.1 (range: 1.4–19.2) for PET positive tumors. All the non-detected tumors had a $TBR_{peak} \leq 1.3$, yielding a cut-off value for detection of $TBR_{peak} \geq 1.4$ (Fig. 3), corresponding to $TBR_{max} \geq 2.0$ (Supplementary Information 2). The mean background uptake ($SUV_{background}$) of *anti*-3- $[^{18}F]$ FACBC in this patient cohort was very low, 0.37 ± 0.12 .

TBR_{peak} increased with malignancy grade in diffuse gliomas, although with overlap between the groups (Fig. 4).

Median TBR_{peak} was 1.2, 2.2, and 8.2 for grade 2, grade 3, and grade 4 gliomas, respectively. There was a significant difference in TBR_{peak} across glioma grades (Kruskal-Wallis test; $p < 0.001$). Pairwise comparisons of TBR_{peak} between different glioma grades showed a significant difference between grade 2 and 4 gliomas ($p < 0.001$), and between grade 3 and 4 gliomas ($p = 0.002$), but not between grade 2 and 3 gliomas ($p = 0.167$) (Fig. 4a). A significant difference was also found between low- (grade 2) and high-grade (grade 3 and 4) gliomas ($p < 0.001$) (Fig. 4b).

Median TBR_{peak} was 1.1, 1.5, and 8.2 for astrocytomas, oligodendrogliomas, and glioblastomas, respectively. There was a significant difference in TBR_{peak} across diffuse glioma types (Kruskal-Wallis test; $p < 0.001$). Pairwise comparisons showed a significant difference in TBR_{peak} between glioblastomas and astrocytomas ($p < 0.001$) and between glioblastomas and oligodendrogliomas ($p < 0.001$), but not between astrocytomas and oligodendrogliomas ($p = 0.842$) (Fig. 5a). There was a significant difference in TBR_{peak} between diffuse IDHwt gliomas and IDH1/2 mutated gliomas ($p < 0.001$) (Fig. 5b). It was not possible to distinguish between grade 2–3 astrocytomas and oligodendrogliomas ($p = 0.370$) (Fig. 5c). No statistical differences in TBR_{peak} were found for primary versus recurrent gliomas ($p = 0.719$) (data not shown).

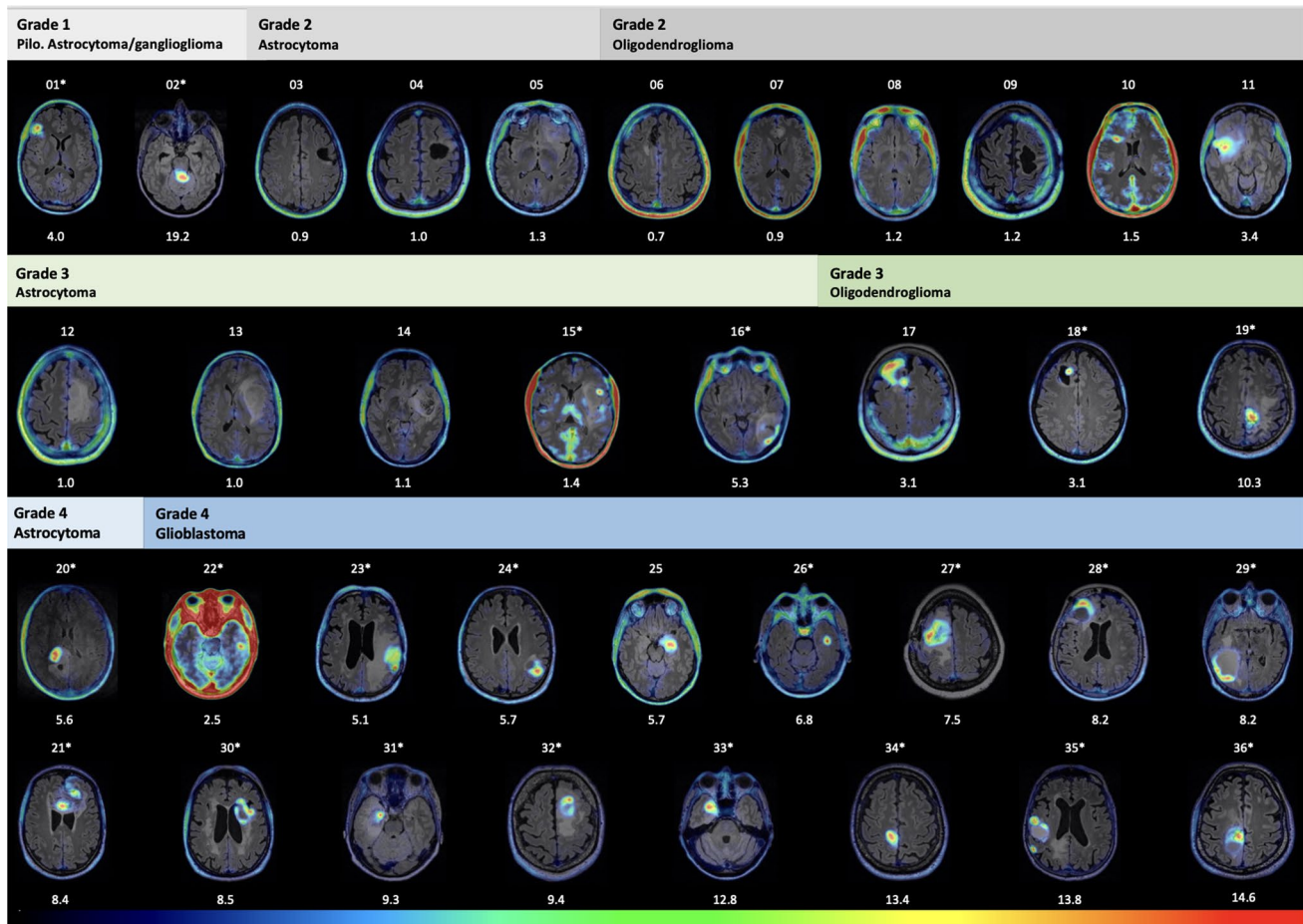


Fig. 2 PET/MR images from all patients sorted by glioma grade and type. Patient ID (from 01 to 36) is shown above — and TBR_{peak} below each image. PET color scale: $SUV_{background}$ to SUV_{max} for PET

From the ROC analyses, threshold values were obtained with the aim to classify different glioma grades, types, and IDH status based on TBR_{peak} values. Grade 2 and grade 4 gliomas could be discriminated from other glioma grades with outstanding and excellent performance, respectively (grade 2: $AUC = 0.91$, 95% CI: 0.82–1.00, $p < 0.001$; grade 4: $AUC = 0.89$, 95% CI 0.76–1.00, $p < 0.001$). TBR_{peak} threshold interval for grade 3 gliomas was defined from the thresholds of grade 2 and 4 gliomas, and AUC for grade 3 can therefore not be defined. For subtypes of gliomas, glioblastomas and diffuse astrocytomas could be discriminated from other gliomas with excellent and acceptable performance, respectively (glioblastoma: $AUC = 0.87$, 95% CI: 0.74–0.99, $p < 0.001$; diffuse astrocytoma: $AUC = 0.78$, 95% CI: 0.62–0.94, $p < 0.010$). TBR_{peak} threshold interval for oligodendrogliomas was defined from the obtained thresholds of glioblastomas and diffuse astrocytomas, and AUC for oligodendrogliomas can therefore not be defined. Furthermore, IDHwt gliomas could be discriminated from IDH-mutated gliomas with outstanding performance ($AUC = 0.91$, 95%

positive tumors and from $SUV_{background}$ to $SUV = 2$ for PET negative tumors. Patients denoted with a star also demonstrated MRI contrast enhancement

CI: 0.81–1.00, $p < 0.001$). Optimal threshold values, sensitivities, and specificities can be found in Table 1.

Dynamic PET analysis

All except one (25/26, 96.2%) of the time-activity curves (TACs) for SUV_{peak} were increasing for a range of glioma types and grades, indicating that dynamic analyses for glioma classification is not useful with *anti-3- ^{18}F FACBC* PET. Only one patient (ID_02, grade 1 pilocytic astrocytoma) had a decreasing curve (data not shown). TBR_{peak} was generally quite stable 10–45 min p.i, suggesting that this is a good interval for imaging. Figure 6 exemplifies TACs for six different glioma types and grades.

Predicted diagnoses with and without *anti-3- ^{18}F FACBC* PET

Characteristics from the systematic MRI readings are presented in Supplementary Information 3. Ring contrast

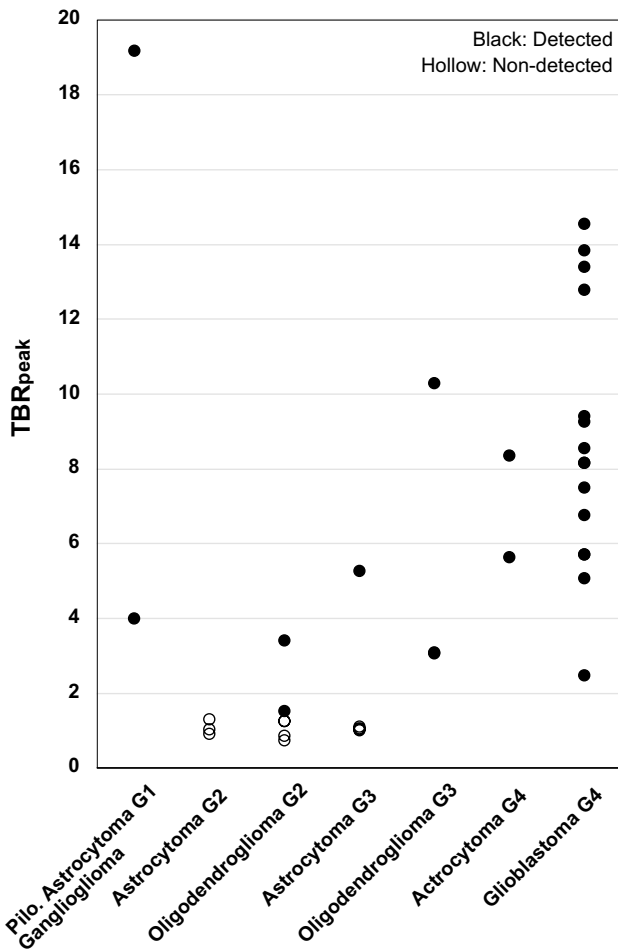
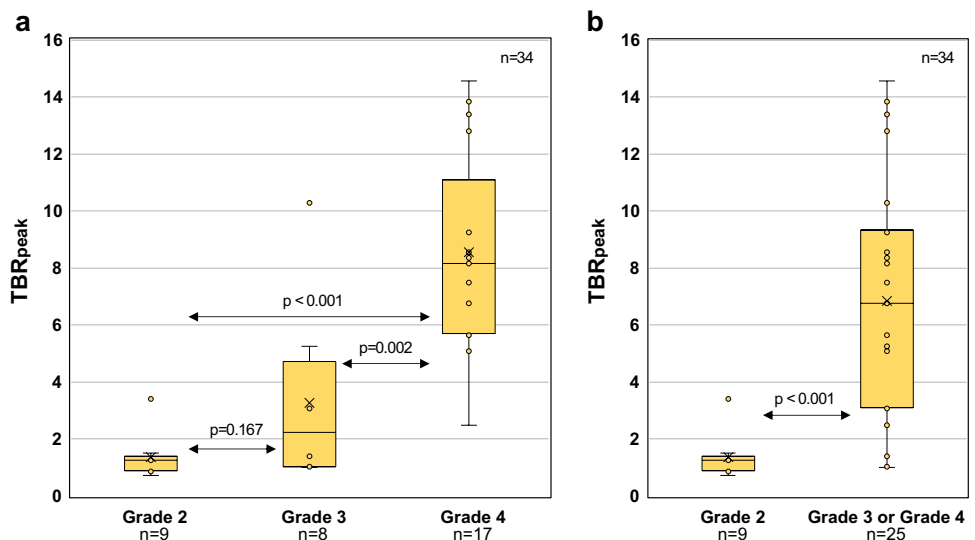


Fig. 3 Peak tumor-to-background ratios (TBR_{peak}) for all patients categorized by tumor type and grade (G). Black dots indicate PET positive and hollow dots PET negative gliomas. Cut-off value for tumor detection was $TBR_{peak} \geq 1.4$

Fig. 4 Peak tumor-to-background ratio (TBR_{peak}) variations for different glioma grades. **a** There was a significant difference between grade 2 and 4 gliomas, and between grade 3 and 4 gliomas, but not between grade 2 and 3 gliomas. **b** A significant difference was also observed between grade 2 and grade 3–4 gliomas



enhancement and central necrosis were defined by both readers with a *strong* inter-rater agreement ($\kappa=0.816, p < 0.001$). T2/FLAIR mismatch had a *moderate* inter-rater agreement ($\kappa = -0.719, p < 0.001$). Other imaging features like predominantly cortical based and patchy contrast enhancement varied more and resulted in a *weak* inter-rater agreement ($\kappa=0.500$ and $\kappa=0.588$, respectively, $p < 0.001$). A *minimal* inter-rater agreement was found for increased rCBV ($\kappa=0.393, p=0.003$). Indirect signs of calcification had *no* inter-rater agreement ($\kappa = -0.038, p=0.806$). A *moderate* inter-rater correlation was found for ADC values ($ICC=0.668, p < 0.001$).

The potential diagnostic accuracy for adding *anti-3-¹⁸F* FACBC PET to MRI were estimated from the established threshold values for different glioma grades, types, and IDH status (Table 1). Adding *anti-3-¹⁸F* FACBC PET to routine MRI sequences improved the proportion of correctly predicted glioma diagnoses, grades, types, and IDH status (Table 2). The diagnostic accuracy improved by 13.9 and 16.7 percentage points for the two readers, respectively.

Discussion

The key finding in this study was that *anti-3-¹⁸F* FACBC PET improved the proportion of correctly predicted glioma grades, types, and IDH status, as well as the overall diagnoses compared to MRI only.

A more trustworthy pretreatment diagnosis can be useful in clinical decision making. For example, asymptomatic grade 1 gliomas may not necessarily need treatment, but may still undergo treatment if mistaken for a higher-grade lesion, like in the current study where two grade 1 gliomas were included since they were scheduled for treatment based on suspicion of being diffuse gliomas (grade 2–4). Furthermore,

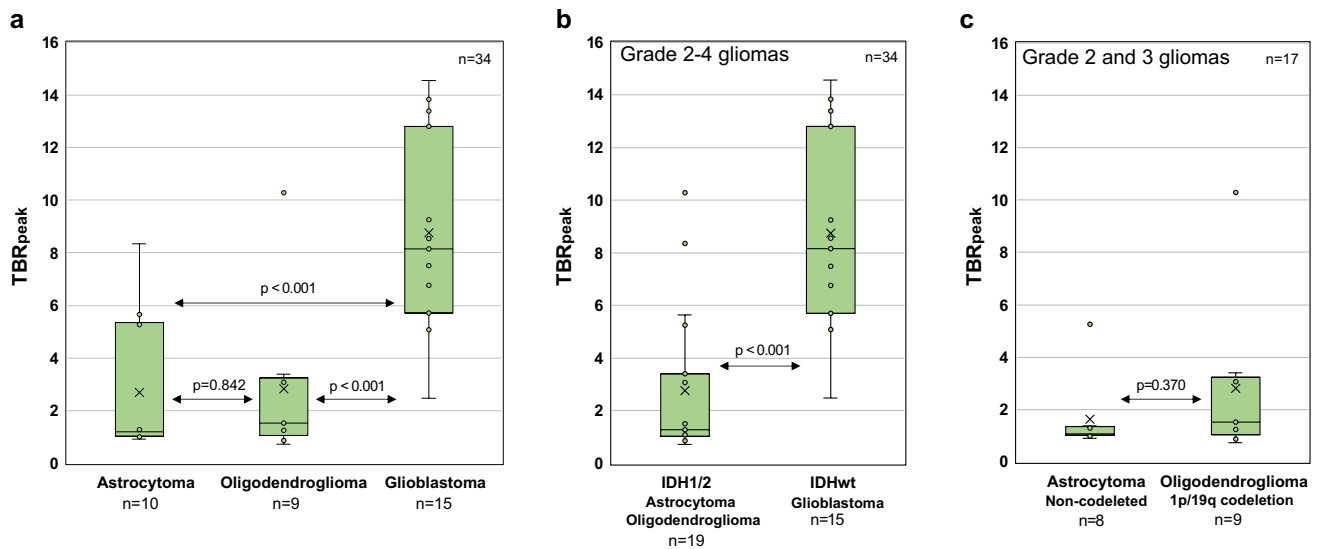


Fig. 5 Peak tumor-to-background ratio (TBR_{peak}) variations for different tumor types and IDH status. **a** There was a significant difference between glioblastomas and astrocytomas/oligodendrogliomas and

between **b** diffuse IDH wildtype gliomas and IDH1/2 mutated gliomas. **c** No significant difference was found between grade 2–3 astrocytomas and oligodendrogliomas

the prognostic difference between grade 4 glioblastomas and grade 2–3 astrocytomas and between grade 2–3 oligodendrogliomas and grade 2–3 astrocytomas could potentially affect surgical decision making. Oligodendrogliomas often exhibit a better response to adjuvant treatment, and the impact of surgery is more documented for astrocytomas [41]. While surgically induced deficits may reduce survival in grade 4 glioblastomas [42], patients with lower grade astrocytomas have far more to gain from extensive resections [43] and have more time for rehabilitation.

It is an advantage that *anti*-3- $[^{18}F]$ FACBC has lower uptake in normal brain parenchyma and thus higher TBR values than other AA tracers [19, 20, 44, 45]. PET hotspots appear very distinct, and in most cases, the regions with PET uptake and contrast-enhancement coincide well. However,

anti-3- $[^{18}F]$ FACBC detected malignancy in 4/14 (30%) of patients where no contrast-enhancement were found on MRI in the current study (two grade 2 oligodendrogliomas, one grade 3 oligodendroglioma, and one grade 4 glioblastoma), suggesting that *anti*-3- $[^{18}F]$ FACBC PET could be particularly useful in cases without contrast-enhancement on MRI.

The overall sensitivity for *anti*-3- $[^{18}F]$ FACBC in detection of gliomas was 72.2%. This is slightly lower than reported from studies using $[^{11}C]$ MET (76–100% (14 studies, $n = 556$) [46]), $[^{18}F]$ FET (89% (1 study, $n = 236$) [47]), and $[^{18}F]$ FDOPA (90–100% (3 studies, $n = 114$) [48–50]). A possible explanation could be that almost 80% of the WHO grade 2 gliomas were PET negative in this study, while for other AAs this is reported to between 20 and 30% [47, 51, 52]. Thus, another advantage with *anti*-3- $[^{18}F]$ FACBC

Table 1 Optimal TBR_{peak} threshold values for differentiation between glioma grades, types, and molecular features, obtained with the ROC-analyses ($n = 36$)

Tumor characteristics	TBR_{peak} threshold	Sensitivity	Specificity	AUC	CI	<i>p</i> -value
Grade 2 (vs other gliomas)	< 2.00	0.89	0.85	0.91	0.82–1.00	< 0.001
Grade 3 (vs other gliomas)	2.00–4.52 ¹	0.25	0.89	x	x	x
Grade 4 (vs other gliomas)	> 4.52	0.94	0.84	0.89	0.76–1.00	< 0.001
Glioblastoma (vs other gliomas)	≥ 5.68	0.87	0.86	0.87	0.74–0.99	< 0.001
Oligodendroglioma (vs other gliomas)	1.45–5.68 ²	0.44	0.81	x	x	x
Diffuse astrocytoma (vs other gliomas)	≤ 1.45	0.70	0.85	0.78	0.62–0.94	0.010
IDHwt (vs IDH1/2)	≥ 3.69	0.94	0.79	0.91	0.81–1.00	< 0.001

¹Defined from thresholds of grade 2 and grade 4 gliomas

²Defined from thresholds of diffuse astrocytomas and glioblastomas

^xNot defined, since TBR_{peak} thresholds for grade 3 gliomas and for oligodendrogliomas are within an interval

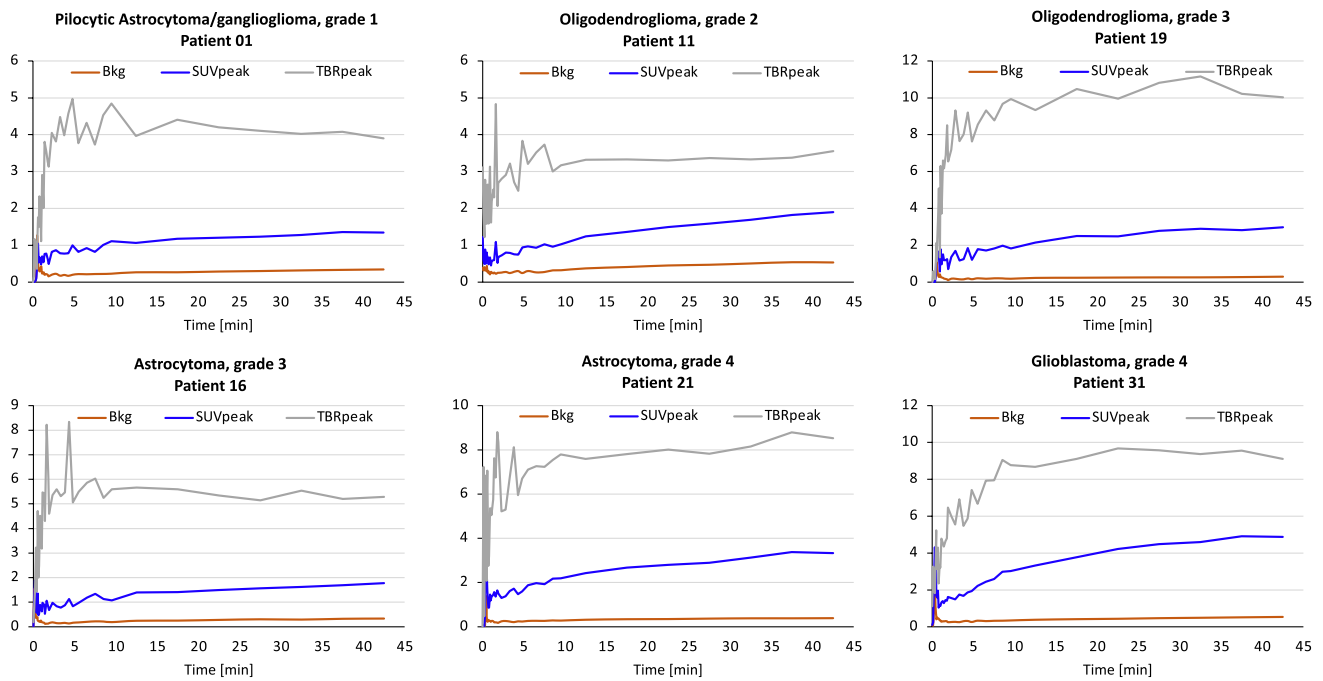


Fig. 6 Examples of time-activity curves from six patients with different glioma types and grades. The similar curve characteristics (increasing) for SUV_{peak} for all tumors indicate that dynamic *anti-*

$3-[^{18}F]FACBC$ PET cannot be used to differentiate between glioma types and grades (Bkg, background)

over the other AAs is a significant difference between the PET uptake in diffuse low-grade and high-grade gliomas (Fig. 4b). Parent et al. [27] also demonstrated that *anti-3-[$^{18}F]FACBC$* PET could discriminate between low- and high-grade glioma, although for a smaller sample size ($n = 18$ and only one grade 3 glioma).

All glioblastomas had uptake in this study, and similar results have been demonstrated for [^{18}F]FET [47]. However, for grade 2–3 astrocytomas and grade 2 oligodendrogliomas, [^{11}C]MET and [^{18}F]FET demonstrate higher sensitivities [47, 53], and are probably better suited than *anti-3-[$^{18}F]FACBC$* for evaluation and follow-up of these subtypes.

The challenge to discriminate grade 2–3 astrocytomas from oligodendrogliomas remains, even though the fraction of PET positives among grade 2–3 oligodendrogliomas

were larger. Oligodendrogliomas, especially grade 3, have a higher AA metabolism compared to IDH-mutated astrocytomas and are most commonly positive at AA PET compared to IDH-mutated astrocytomas, as demonstrated both in this study and by Ninatti et al. [54]. In this study, the group of included grade 2 oligodendrogliomas is larger than the group of grade 2 astrocytomas, and the group of grade 3 astrocytomas is larger than the group of grade 3 oligodendrogliomas. Consequently, this unbalance may have masked statistical differences in *anti-3-[$^{18}F]FACBC$* uptake values between these glioma subtypes.

IDH mutation is one of the most important diagnostic and prognostic biomarkers for diffuse gliomas and is associated with a more favorable outcome compared to IDHwt [55]. When comparing TBR_{peak} between diffuse IDHwt and

Table 2 Predicted glioma grade, type, IDH status, and diagnosis by two readers with MRI alone and MRI supplemented with *anti-3-[$^{18}F]FACBC$* PET

Accuracy	MRI only		MRI+PET		Improvement with PET	
	Reader 1 (%)	Reader 2 (%)	Reader 1 (%)	Reader 2 (%)	Reader 1 (p.p.)	Reader 2 (p.p.)
Correct grade	66.7	75.0	77.8	83.3	11.1	8.3
Correct type	61.1	66.7	77.8	77.8	16.7	11.1
Correct IDH status	80.6	80.6	91.7	88.9	11.1	8.3
Correct diagnosis (grade and type)	47.2	55.6	63.9	69.4	16.7	13.9

IDH1/2 mutated gliomas, we found that IDHwt gliomas had a significantly higher uptake compared to IDH1/2 mutated gliomas. Similar results have also been demonstrated by Kudulaiti et al. [56] for [^{11}C]MET. Additionally, [^{18}F]FET and [^{18}F]FDOPA shows potential as effective tools to predict IDH genotype in gliomas using radiomics with static and dynamic PET parameters [57, 58].

Grade 4 glioblastomas and the grade 1 gliomas were among the tumors with the highest uptake of *anti*-3- ^{18}F FACBC, and all of them were PET positive. Common for these tumors are that they are IDHwt. This high uptake is not necessarily caused by the IDH status but could be related to the increased vascular proliferation found in both grade 1 and 4 gliomas [59], which would also explain the high uptake in the two grade 4 IDH mutated astrocytomas in this study.

It has been suggested that the dynamic characteristics of AA PET can be useful in the classification of gliomas. However, the dynamic characteristics found with [^{18}F]FET (increasing curve for low-grade tumors, decreasing curve for high-grade tumors) [60] and with [^{18}F]FDOPA (to predict molecular features) [61, 62] could not be established with *anti*-3- ^{18}F FACBC in this study. Accordingly, dynamic imaging with *anti*-3- ^{18}F FACBC is probably not useful for glioma classification. However, it may still be relevant to evaluate this tracer dynamically in a follow-up setting to differentiate between recurrence and treatment-induced changes. Differences in dynamic characteristics between the tracers are probably caused by different uptake and transport mechanisms (*anti*-3- ^{18}F FACBC: System L and ASCT2 transport, and [^{11}C]MET: System L (LAT1) transport/protein synthesis, [^{18}F]FET: System L (LAT1) transport, and [^{18}F]FDOPA: System L (LAT1) transport) [16, 21, 22].

By applying different TBR_{peak} threshold values, we could discriminate some glioma grades, types, and molecular features from others with excellent or outstanding performance (grade 2, grade 4, glioblastoma, and IDHwt). Oligodendrogliomas or diffuse astrocytomas could be discriminated from other gliomas with acceptable performance, where the lower performance may be caused by quite similar uptake between these two subtypes and the wide range in uptake for grade 2–4 astrocytomas. A limitation with this ROC analysis was the small sample size, which also made it impossible to split the data into training and test cohorts. This resulted most likely in overestimation of the test performance [63]. However, by applying the obtained threshold values from *anti*-3- ^{18}F FACBC PET, the accuracy of the predicted glioma diagnoses improved compared to MRI alone for both readers. The importance to also include the grade 1 gliomas in the ROC analysis was confirmed in the retrospective clinical MR readings, where these two tumors were predicted to be grade 3 astrocytomas by one (patient ID_02) or both (patient ID_01) of the neuroradiologists. It is, however, important

to be aware that this methodological choice influence comparability with studies that aim to include only adult-type diffuse gliomas.

The reference standard was histomolecular diagnoses based on the latest 2021 WHO classification of CNS tumors. It should be noted that this classification differs from previous versions, with the most important changes being more incorporation of molecular biomarkers for tumor classification. Tumors are further graded within types, rather than across different tumor types [7]. Applying a more robust classification system will likely improve the evaluation of diagnostic imaging as well. According to the 2021 WHO classification, all IDH mutated diffuse, astrocytic, grade 2 and 3 gliomas should be tested for CDKN2A/B homozygous deletion, since the presence of this marker would assign a grade 4 glioma [6, 7]. This was however not performed systematically in the current study, and must therefore be acknowledged as a limitation, even if the frequencies of this marker are low in astrocytic gliomas (grade 2: 0–12%; grade 3: 6–20%) [64].

An overall limitation is the relatively small patient cohort. However, by merging new data with data from our previously published data [24], we were able to perform one of the largest studies using *anti*-3- ^{18}F FACBC in gliomas so far.

Conclusions

This study demonstrates that the majority of gliomas are *anti*-3- ^{18}F FACBC avid tumors and that the uptake increases with malignancy grade for diffuse gliomas. *Anti*-3- ^{18}F FACBC PET could be a valuable tool to discriminate grade 2 gliomas, grade 4 gliomas, glioblastomas, and IDHwt gliomas from other gliomas. Combined *anti*-3- ^{18}F FACBC PET/MRI improved the accuracy of the predicted glioma grades, types, and IDH status, as well as the overall diagnostic accuracy compared to conventional MRI alone. This tracer should be considered as an alternative to other recommended AA tracers for glioma imaging.

Supplementary Information The online version contains supplementary material available at <https://doi.org/10.1007/s00259-023-06437-4>.

Acknowledgements The authors would like to thank technicians and research coordinators at St. Olavs Hospital, Trondheim University Hospital, and University of North Norway, Tromsø. We thank Jon André Totland at the University of North Norway, Tromsø. We also thank Trond Mohn Foundation within the Norwegian Nuclear Medicine Consortium (180°N), Central Norway Regional Health Authority, and Fondstiftelsen at St. Olavs Hospital for funding this study.

Author contribution Live Eikenes and Anna Karlberg conceived and designed the study with the participation of Erik Magnus Berntsen and Tor Ingebrigtsen. Live Eikenes and Anna Karlberg were responsible for the implementation of the study. Ole Solheim and Lars Kjelsberg

Pedersen were responsible for patient recruitment. Material preparation and data analysis were mainly performed by Anna Karlberg with the assistance of Benedikte Emilie Vindstad. Initial MRI readings were performed by Erik Magnus Berntsen. Kjell Arne Kvistad and Karoline Skogen did the systematic, retrospective MRI readings. PET readings were performed by Håkon Johansen and Trond Velde Bogsrud. Anne Jarstein Skjulsvik and Kristin Smistad Myrmed did the histomolecular analyses. Guro F. Giskeødegård assisted with statistical calculations. The first draft of the manuscript was written by Anna Karlberg with assistance from Lars Kjelsberg Pedersen. All authors revised the manuscript critically and read and approved the final manuscript.

Funding Open access funding provided by NTNU Norwegian University of Science and Technology (incl St. Olavs Hospital - Trondheim University Hospital) This study was funded by the Trond Mohn Foundation within the Norwegian Nuclear medicine Consortium (180°N) (<https://www.ntnu.edu/180n>), Central Norway Regional Health Authority, and Fondstiftelsen at St. Olavs Hospital.

Data availability The datasets generated and/or analyzed during the current study are not publicly available due to the European Union General Data Protection Regulations (GDPR), but are available from the corresponding author on reasonable request.

Declarations

Study protocol The study protocol is available from the corresponding author on reasonable request.

Ethics approval The study was approved by the Regional Ethics Committee (REC Central Norway, reference numbers 2016/279 and 2018/2243).

Consent to participate Informed consent was obtained from all individual participants included in the study.

Consent for publication The authors affirm that human research participants provided informed consent for publication of the images in Fig. 2.

Competing interests The authors declare no competing interests.

Open Access This article is licensed under a Creative Commons Attribution 4.0 International License, which permits use, sharing, adaptation, distribution and reproduction in any medium or format, as long as you give appropriate credit to the original author(s) and the source, provide a link to the Creative Commons licence, and indicate if changes were made. The images or other third party material in this article are included in the article's Creative Commons licence, unless indicated otherwise in a credit line to the material. If material is not included in the article's Creative Commons licence and your intended use is not permitted by statutory regulation or exceeds the permitted use, you will need to obtain permission directly from the copyright holder. To view a copy of this licence, visit <http://creativecommons.org/licenses/by/4.0/>.

References


- Ostrom QT, Price M, Neff C, Cioffi G, Waite KA, Kruchko C, et al. CBTRUS statistical report: primary brain and other central nervous system tumors diagnosed in the United States in 2015–2019. *Neuro Oncol.* 2022;24:v1–95. <https://doi.org/10.1093/neuonc/noac202>.
- Schwartzbaum JA, Fisher JL, Aldape KD, Wrensch M. Epidemiology and molecular pathology of glioma. *Nat Clin Pract Neurol.* 2006;2:494–503; quiz 1 p following 16. <https://doi.org/10.1038/ncpneuro0289>.
- Voisin MR, Sasikumar S, Mansouri A, Zadeh G. Incidence and prevalence of primary malignant brain tumours in Canada from 1992 to 2017: an epidemiologic study. *CMAJ Open.* 2021;9:E973–9. <https://doi.org/10.9778/cmajo.20200295>.
- Lin D, Wang M, Chen Y, Gong J, Chen L, Shi X, et al. Trends in intracranial glioma incidence and mortality in the United States, 1975–2018. *Front Oncol.* 2021;11:748061. <https://doi.org/10.3389/fonc.2021.748061>.
- Årsrapport 2022 med resultater og forbedringstiltak fra Kvalitetsregister for hjerne- og ryggmargssvulster [Annual Report 2022 Brain and spinal cord tumors] Oslo: Cancer Registry of Norway. [Norwegian]. 2023.
- WHO Classification of Tumours Editorial Board. World Health Organization Classification of Tumours of the Central Nervous System. 5th ed. Lyon: International Agency for Research on Cancer; 2021.
- Louis DN, Perry A, Wesseling P, Brat DJ, Cree IA, Figarella-Branger D, et al. The 2021 WHO Classification of Tumors of the Central Nervous System: a summary. *Neuro Oncol.* 2021;23:1231–51. <https://doi.org/10.1093/neuonc/noab106>.
- Halasz LM, Attia A, Bradfield L, Brat DJ, Kirkpatrick JP, Laack NN, et al. Radiation therapy for IDH-mutant grade 2 and grade 3 diffuse glioma: an ASTRO clinical practice guideline. *Pract Radiat Oncol.* 2022;12:370–86. <https://doi.org/10.1016/j.prro.2022.05.004>.
- Weller M, van den Bent M, Preusser M, Le Rhun E, Tonn JC, Minniti G, et al. EANO guidelines on the diagnosis and treatment of diffuse gliomas of adulthood. *Nat Rev Clin Oncol.* 2021;18:170–86. <https://doi.org/10.1038/s41571-020-00447-z>.
- Ellingson BM, Bendszus M, Boxerman J, Barboriak D, Erickson BJ, Smits M, et al. Consensus recommendations for a standardized Brain Tumor Imaging Protocol in clinical trials. *Neuro Oncol.* 2015;17:1188–98. <https://doi.org/10.1093/neuonc/nov095>.
- Fouke SJ, Benzinger T, Gibson D, Ryken TC, Kalkanis SN, Olson JJ. The role of imaging in the management of adults with diffuse low grade glioma: a systematic review and evidence-based clinical practice guideline. *J Neurooncol.* 2015;125:457–79. <https://doi.org/10.1007/s11060-015-1908-9>.
- Chandrasoma PT, Smith MM, Apuzzo ML. Stereotactic biopsy in the diagnosis of brain masses: comparison of results of biopsy and resected surgical specimen. *Neurosurgery.* 1989;24:160–5. <https://doi.org/10.1227/00006123-198902000-00002>.
- Feiden W, Steude U, Bise K, Gundisch O. Accuracy of stereotactic brain tumor biopsy: comparison of the histologic findings in biopsy cylinders and resected tumor tissue. *Neurosurg Rev.* 1991;14:51–6. <https://doi.org/10.1007/BF00338192>.
- Paulus W, Peiffer J. Intratumoral histologic heterogeneity of gliomas. A quantitative study. *Cancer.* 1989;64:442–7. [https://doi.org/10.1002/1097-0142\(19890715\)64:2<442::aid-cnrc2820640217>3.0.co;2-s](https://doi.org/10.1002/1097-0142(19890715)64:2<442::aid-cnrc2820640217>3.0.co;2-s).
- Huang C, McConathy J. Radiolabeled amino acids for oncologic imaging. *J Nucl Med.* 2013;54:1007–10. <https://doi.org/10.2967/jnumed.112.113100>.
- Sun A, Liu X, Tang G. Carbon-11 and fluorine-18 labeled amino acid tracers for positron emission tomography imaging of tumors. *Front Chem.* 2017;5:124. <https://doi.org/10.3389/fchem.2017.00124>.
- Albert NL, Weller M, Suchorska B, Galldiks N, Soffietti R, Kim MM, et al. Response assessment in neuro-oncology working group and European Association for Neuro-Oncology recommendations

- for the clinical use of PET imaging in gliomas. *Neuro Oncol.* 2016;18:1199–208. <https://doi.org/10.1093/neuonc/now058>.
18. Law I, Albert NL, Arbizu J, Boellaard R, Drzezga A, Galldiks N, et al. Joint EANM/EANO/RANO practice guidelines/SNMMI procedure standards for imaging of gliomas using PET with radiolabelled amino acids and [(18)F]FDG: version 1.0. *Eur J Nucl Med Mol Imaging.* 2019;46:540–57. <https://doi.org/10.1007/s00259-018-4207-9>.
 19. Michaud L, Beattie BJ, Akhurst T, Dunphy M, Zanzonico P, Finn R, et al. (18)F-Fluciclovine ((18)F-FACBC) PET imaging of recurrent brain tumors. *Eur J Nucl Med Mol Imaging.* 2020;47:1353–67. <https://doi.org/10.1007/s00259-019-04433-1>.
 20. Tsuyuguchi N, Terakawa Y, Uda T, Nakajo K, Kanemura Y. Diagnosis of brain tumors using amino acid transport PET imaging with (18)F-fluciclovine: a comparative study with L-methyl-(11) C-methionine PET imaging. *Asia Ocean J Nucl Med Biol.* 2017;5:85–94. <https://doi.org/10.22038/aojnmb.2017.8843>.
 21. Habermeier A, Graf J, Sandhofer BF, Boissel JP, Roesch F, Closs EI. System L amino acid transporter LAT1 accumulates O-(2-fluoroethyl)-L-tyrosine (FET). *Amino Acids.* 2015;47:335–44. <https://doi.org/10.1007/s00726-014-1863-3>.
 22. Oka S, Okudaira H, Ono M, Schuster DM, Goodman MM, Kawai K, et al. Differences in transport mechanisms of trans-1-amino-3-[18F]fluorocyclobutanecarboxylic acid in inflammation, prostate cancer, and glioma cells: comparison with L-[methyl-11C]methionine and 2-deoxy-2-[18F]fluoro-D-glucose. *Mol Imaging Biol.* 2014;16:322–9. <https://doi.org/10.1007/s11307-013-0693-0>.
 23. Bogsrud TV, Londalen A, Brandal P, Leske H, Panagopoulos I, Borghammer P, et al. 18F-Fluciclovine PET/CT in suspected residual or recurrent high-grade glioma. *Clin Nucl Med.* 2019;44:605–11. <https://doi.org/10.1097/RLU.0000000000002641>.
 24. Karlberg A, Berntsen EM, Johansen H, Skjulsvik AJ, Reinertsen I, Dai HY, et al. 18F-FACBC PET/MRI in diagnostic assessment and neurosurgery of gliomas. *Clin Nucl Med.* 2019;44:550–9. <https://doi.org/10.1097/RLU.0000000000002610>.
 25. Kondo A, Ishii H, Aoki S, Suzuki M, Nagasawa H, Kubota K, et al. Phase IIa clinical study of [(18)F]fluciclovine: efficacy and safety of a new PET tracer for brain tumors. *Ann Nucl Med.* 2016;30:608–18. <https://doi.org/10.1007/s12149-016-1102-y>.
 26. Wakabayashi T, Iuchi T, Tsuyuguchi N, Nishikawa R, Arakawa Y, Sasayama T, et al. Diagnostic performance and safety of positron emission tomography using (18)F-fluciclovine in patients with clinically suspected high- or low-grade gliomas: a multicenter phase IIb trial. *Asia Ocean J Nucl Med Biol.* 2017;5:10–21. <https://doi.org/10.22038/aojnmb.2016.7869>.
 27. Parent EE, Benayoun M, Ibeanu I, Olson JJ, Hadjipanayis CG, Brat DJ, et al. [F-18]Fluciclovine PET discrimination between high- and low-grade gliomas. *Ejnmri Res.* 2018;8. ARTN 67. <https://doi.org/10.1186/s13550-018-0415-3>.
 28. Shoup TM, Olson J, Hoffman JM, Votaw J, Eshima D, Eshima L, et al. Synthesis and evaluation of [18F]1-amino-3-fluorocyclobutane-1-carboxylic acid to image brain tumors. *J Nucl Med.* 1999;40:331–8.
 29. Laudicella R, Albano D, Alongi P, Argiroffi G, Bauckneht M, Baldari S, et al. (18)F-Facbc in prostate cancer: a systematic review and meta-analysis. *Cancers (Basel).* 2019;11:1348. <https://doi.org/10.3390/cancers11091348>.
 30. Bossuyt PM, Reitsma JB, Bruns DE, Gatsonis CA, Glasziou PP, Irwig L, et al. STARD 2015: an updated list of essential items for reporting diagnostic accuracy studies. *BMJ.* 2015;351:h5527. <https://doi.org/10.1136/bmj.h5527>.
 31. Ladefoged CN, Hansen AE, Henriksen OM, Bruun FJ, Eikenes L, Oen SK, et al. AI-driven attenuation correction for brain PET/MRI: clinical evaluation of a dementia cohort and importance of the training group size. *Neuroimage.* 2020;222:117221. <https://doi.org/10.1016/j.neuroimage.2020.117221>.
 32. Ladefoged CN, Marner L, Hindsholm A, Law I, Hojgaard L, Andersen FL. Deep learning based attenuation correction of PET/MRI in pediatric brain tumor patients: evaluation in a clinical setting. *Front Neurosci.* 2018;12:1005. <https://doi.org/10.3389/fnins.2018.01005>.
 33. Johnson DR, Giannini C, Vaubel RA, Morris JM, Eckel LJ, Kaufmann TJ, et al. A radiologist's guide to the 2021 WHO Central Nervous System Tumor Classification: part I—key concepts and the spectrum of diffuse gliomas. *Radiology.* 2022;304:494–508. <https://doi.org/10.1148/radiol.213063>.
 34. Kamble AN, Agrawal NK, Koundal S, Bhargava S, Kamble AN, Joyner DA, et al. Imaging-based stratification of adult gliomas prognosticates survival and correlates with the 2021 WHO classification. *Neuroradiology.* 2023;65:41–54. <https://doi.org/10.1007/s00234-022-03015-7>.
 35. McNamara C, Mankad K, Thust S, Dixon L, Limback-Stanic C, D'Arco F, et al. 2021 WHO classification of tumours of the central nervous system: a review for the neuroradiologist. *Neuroradiology.* 2022;64:1919–50. <https://doi.org/10.1007/s00234-022-03008-6>.
 36. Unterrainer M, Vettermann F, Brendel M, Holzgreve A, Lifschitz M, Zahringer M, et al. Towards standardization of (18)F-FET PET imaging: do we need a consistent method of background activity assessment? *EJNMMI Res.* 2017;7:48. <https://doi.org/10.1186/s13550-017-0295-y>.
 37. McHugh ML. Interrater reliability: the kappa statistic. *Biochem Med (Zagreb).* 2012;22:276–82.
 38. Koo TK, Li MY. A guideline of selecting and reporting intraclass correlation coefficients for reliability research. *J Chiropr Med.* 2016;15:155–63. <https://doi.org/10.1016/j.jcm.2016.02.012>.
 39. Hosmer JRDW, Lemeshow S, Sturdivant RX. *Applied logistic regression.* 3rd ed. Hoboken, New Jersey: Wiley & Sons, Inc.; 2013.
 40. Karlberg A, Berntsen EM, Johansen H, Myrthue M, Skjulsvik AJ, Reinertsen I, et al. Multimodal (18)F-fluciclovine PET/MRI and ultrasound-guided neurosurgery of an anaplastic oligodendroglioma. *World Neurosurg.* 2017;108(989):e1–8. <https://doi.org/10.1016/j.wneu.2017.08.085>.
 41. Jakola AS, Pedersen LK, Skjulsvik AJ, Myrmel K, Sjavik K, Solheim O. The impact of resection in IDH-mutant WHO grade 2 gliomas: a retrospective population-based parallel cohort study. *J Neurosurg.* 2022;137:1321–8. <https://doi.org/10.3171/2022.1.JNS212514>.
 42. Aabedi AA, Young JS, Zhang Y, Ammanuel S, Morshed RA, Dalle Ore C, et al. Association of neurological impairment on the relative benefit of maximal extent of resection in chemoradiation-treated newly diagnosed isocitrate dehydrogenase wild-type glioblastoma. *Neurosurgery.* 2022;90:124–30. <https://doi.org/10.1227/NEU.0000000000001753>.
 43. Kavouridis VK, Boaro A, Dorr J, Cho EY, Iorgulescu JB, Reardon DA, et al. Contemporary assessment of extent of resection in molecularly defined categories of diffuse low-grade glioma: a volumetric analysis. *J Neurosurg.* 2019;133:1291–301. <https://doi.org/10.3171/2019.6.JNS19972>.
 44. Grosu AL, Astner ST, Riedel E, Nieder C, Wiedenmann N, Heinemann F, et al. An interindividual comparison of O-(2-[18F]fluoroethyl)-L-tyrosine (FET)- and L-[methyl-11C]methionine (MET)-PET in patients with brain gliomas and metastases. *Int J Radiat Oncol Biol Phys.* 2011;81:1049–58. <https://doi.org/10.1016/j.ijrobp.2010.07.002>.
 45. Lapa C, Linsenmann T, Monoranu CM, Samnick S, Buck AK, Bluemel C, et al. Comparison of the amino acid tracers 18F-FET and 18F-DOPA in high-grade glioma patients. *J Nucl Med.* 2014;55:1611–6. <https://doi.org/10.2967/jnumed.114.140608>.
 46. Glaudemans AW, Enting RH, Heesters MA, Dierckx RA, van Rheenen RW, Walenkamp AM, et al. Value of 11C-methionine PET in imaging brain tumours and metastases. *Eur J Nucl*

- Med Mol Imaging. 2013;40:615–35. <https://doi.org/10.1007/s00259-012-2295-5>.
47. Hutterer M, Nowosielski M, Putzer D, Jansen NL, Seiz M, Schocke M, et al. [18F]-fluoro-ethyl-L-tyrosine PET: a valuable diagnostic tool in neuro-oncology, but not all that glitters is glioma. *Neuro Oncol*. 2013;15:341–51. <https://doi.org/10.1093/neuonc/nos300>.
 48. Ledezma CJ, Chen W, Sai V, Freitas B, Cloughesy T, Czernin J, et al. 18F-FDOPA PET/MRI fusion in patients with primary/recurrent gliomas: initial experience. *Eur J Radiol*. 2009;71:242–8. <https://doi.org/10.1016/j.ejrad.2008.04.018>.
 49. Pafundi DH, Laack NN, Youland RS, Parney IF, Lowe VJ, Gianini C, et al. Biopsy validation of 18F-DOPA PET and biodistribution in gliomas for neurosurgical planning and radiotherapy target delineation: results of a prospective pilot study. *Neuro Oncol*. 2013;15:1058–67. <https://doi.org/10.1093/neuonc/not002>.
 50. Tripathi M, Sharma R, D'Souza M, Jaimini A, Panwar P, Varshney R, et al. Comparative evaluation of F-18 FDOPA, F-18 FDG, and F-18 FLT-PET/CT for metabolic imaging of low grade gliomas. *Clin Nucl Med*. 2009;34:878–83. <https://doi.org/10.1097/RLU.0b013e3181becfe0>.
 51. Jansen NL, Graute V, Armbruster L, Suchorska B, Lutz J, Eigenbrod S, et al. MRI-suspected low-grade glioma: is there a need to perform dynamic FET PET? *Eur J Nucl Med Mol Imaging*. 2012;39:1021–9. <https://doi.org/10.1007/s00259-012-2109-9>.
 52. Werner JM, Lohmann P, Fink GR, Langen KJ, Galldiks N. Current landscape and emerging fields of PET imaging in patients with brain tumors. *Molecules*. 2020;25:1471. <https://doi.org/10.3390/molecules25061471>.
 53. Herholz K, Holzer T, Bauer B, Schroder R, Voges J, Ernestus RI, et al. 11C-methionine PET for differential diagnosis of low-grade gliomas. *Neurology*. 1998;50:1316–22. <https://doi.org/10.1212/wnl.50.5.1316>.
 54. Ninatti G, Sollini M, Bono B, Gozzi N, Fedorov D, Antunovic L, et al. Preoperative [11C]methionine PET to personalize treatment decisions in patients with lower-grade gliomas. *Neuro Oncol*. 2022;24:1546–56. <https://doi.org/10.1093/neuonc/noac040>.
 55. Sharma N, Mallela AN, Shi DD, Tang LW, Abou-Al-Shaar H, Gersey ZC, et al. Isocitrate dehydrogenase mutations in gliomas: a review of current understanding and trials. *Neurooncol Adv*. 2023;5:vdad053. <https://doi.org/10.1093/noajnl/vdad053>.
 56. Kudulaiti N, Zhang H, Qiu T, Lu J, Aibaidula A, Zhang Z, et al. The relationship between IDH1 mutation status and metabolic imaging in nonenhancing supratentorial diffuse gliomas: a (11)C-MET PET study. *Mol Imaging*. 2019;18:1536012119894087. <https://doi.org/10.1177/1536012119894087>.
 57. Lohmann P, Lerche C, Bauer EK, Steger J, Stoffels G, Blau T, et al. Predicting IDH genotype in gliomas using FET PET radiomics. *Sci Rep*. 2018;8:13328. <https://doi.org/10.1038/s41598-018-31806-7>.
 58. Zaragori T, Oster J, Roch V, Hossu G, Chawki MB, Grignon R, et al. (18)F-FDOPA PET for the noninvasive prediction of glioma molecular parameters: a radiomics study. *J Nucl Med*. 2022;63:147–57. <https://doi.org/10.2967/jnumed.120.261545>.
 59. Gi T, Sato Y, Tokumitsu T, Yamashita A, Moriguchi-Goto S, Takeshima H, et al. Microvascular proliferation of brain metastases mimics glioblastomas in squash cytology. *Cytopathology*. 2017;28:228–34. <https://doi.org/10.1111/cyt.12405>.
 60. la Fougere C, Suchorska B, Bartenstein P, Kreth FW, Tonn JC. Molecular imaging of gliomas with PET: opportunities and limitations. *Neuro Oncol*. 2011;13:806–19. <https://doi.org/10.1093/neuonc/nor054>.
 61. Ginet M, Zaragori T, Marie PY, Roch V, Gauchotte G, Rech F, et al. Integration of dynamic parameters in the analysis of (18)F-FDOPA PET imaging improves the prediction of molecular features of gliomas. *Eur J Nucl Med Mol Imaging*. 2020;47:1381–90. <https://doi.org/10.1007/s00259-019-04509-y>.
 62. Zaragori T, Doyen M, Rech F, Blonski M, Taillandier L, Imbert L, et al. Dynamic (18)F-FDopa PET imaging for newly diagnosed gliomas: is a semiquantitative model sufficient? *Front Oncol*. 2021;11:735257. <https://doi.org/10.3389/fonc.2021.735257>.
 63. Cilluffo G, Fasola S, Ferrante G, Montalbano L, Baiardini I, Indinimeo L, et al. Overrating classifier performance in ROC analysis in the absence of a test set: evidence from simulation and Italian CARATkids validation. *Methods Inf Med*. 2019;58:e27–42. <https://doi.org/10.1055/s-0039-1693732>.
 64. Brat DJ, Aldape K, Colman H, Figarella-Branger D, Fuller GN, Giannini C, et al. cIMPACT-NOW update 5: recommended grading criteria and terminologies for IDH-mutant astrocytomas. *Acta Neuropathol*. 2020;139:603–8. <https://doi.org/10.1007/s00401-020-02127-9>.

Publisher's note Springer Nature remains neutral with regard to jurisdictional claims in published maps and institutional affiliations.

Authors and Affiliations

Anna Karlberg^{1,2}  · Lars Kjelsberg Pedersen³ · Benedikte Emilie Vindstad² · Anne Jarstein Skjulsvik^{4,5} · Håkon Johansen¹ · Ole Solheim^{6,7} · Karoline Skogen⁸ · Kjell Arne Kvistad¹ · Trond Velde Bogsrud^{9,10} · Kristin Smistad Myrnes¹¹ · Guro F. Giskeødegård¹² · Tor Ingebrigtsen^{3,13} · Erik Magnus Berntsen^{1,2} · Live Eikenes²

¹ Department of Radiology and Nuclear Medicine, St. Olavs Hospital, Trondheim University Hospital, Prinsesse Kristinas gate 3, N-7030 Trondheim, Norway

² Department of Circulation and Medical Imaging, Norwegian University of Science and Technology, Trondheim, Norway

³ Department of Neurosurgery, University Hospital of North Norway, Tromsø, Norway

⁴ Department of Pathology, St. Olavs Hospital, Trondheim University Hospital, Trondheim, Norway

⁵ Department of Clinical and Molecular Medicine, Faculty of Medical and Health Sciences, Norwegian University of Science and Technology, Trondheim, Norway

⁶ Department of Neurosurgery, St. Olavs Hospital, Trondheim University Hospital, Trondheim, Norway

⁷ Department of Neuroscience, Norwegian University of Science and Technology, Trondheim, Norway

⁸ Department of Radiology and Nuclear Medicine, Oslo University Hospitals, Oslo, Norway

⁹ PET-Centre, University Hospital of North Norway, Tromsø, Norway

¹⁰ Department of Nuclear Medicine and PET-Centre, Aarhus University Hospital, Aarhus, Denmark

¹¹ Department of Pathology, University Hospital of North Norway, Tromsø, Norway

¹² Department of Public Health and Nursing, Norwegian University of Science and Technology, Trondheim, Norway

¹³ Department of Clinical Medicine, Faculty of Health Sciences, UiT the Arctic University of Norway, Tromsø, Norway